CAMBRIDGE
UNIVERSITY PRESS

Article

Middlebackite, a new Cu oxalate mineral from Iron Monarch, South Australia: Description and crystal structure

Peter Elliott[1,2]*

[1]Department of Earth Sciences, School of Physical Sciences, The University of Adelaide, Adelaide, South Australia 5005, Australia; and [2]South Australian Museum, North Terrace, Adelaide, South Australia 5000, Australia

Abstract

Middlebackite is a new supergene mineral formed in the upper levels of the Iron Monarch quarry, South Australia. It occurs as aggregates of blue, prismatic crystals up to 0.3 mm across comprising individual crystals up to 0.05 mm in length associated with atacamite and mottramite. Crystals are translucent with a vitreous lustre and have a pale blue streak. Middlebackite is brittle with one perfect cleavage and uneven fracture. Mohs hardness is ∼2. The calculated density is 3.64 g cm^{-3}. Crystals are biaxial (+) with $\alpha = 1.663(4)$, $\beta = 1.748(4)$ and $\gamma = 1.861(4)$ (measured in white light). The calculated 2V is 86.7°. Pleochroism is X = colourless, Y = very pale blue and Z = dark sky blue; $Z > Y > X$. The empirical formula unit, based on six oxygen atoms per formula unit is $Cu_{2.00}(C_2O_4)Cl_{0.02}(OH)_{1.98}$. Middlebackite is monoclinic, space group $P2_1/c$ with $a = 7.2597(15)$, $b = 5.7145(11)$, $c = 5.6624(11)$ Å, $\beta = 104.20(3)°$, $V = 227.73(8)$ Å^3 and $Z = 2$. The five strongest lines in the powder X-ray diffraction pattern are [d(Å), (I), (hkl)]: 7.070 (16) (100), 3.739 (100) (11$\bar{1}$), 2.860 (18) (020), 2.481 (12) (12$\bar{1}$) and 2.350 (9) (300). The crystal structure was refined from synchrotron single-crystal X-ray diffraction data to $R_1 = 0.0341$ for 596 observed reflections with $F_0 > 4\sigma(F_0)$. The structure is based on sheets of edge- and corner-sharing octahedra parallel to the bc plane. Sheets link in the a direction via oxalate anions.

Introduction

The iron ore deposits in the Middleback Range of South Australia, have been worked since the early 1900s. They were first developed by Broken Hill Proprietary Limited as a source of flux for the lead smelting works at Port Pirie and later mined as a source of iron ore for steel making. Iron Monarch is the largest of the deposits, having produced over 150 million tons of ore. The principal ore mineral is hematite, which grades into siliceous banded iron formation (Milnes, 1954). The upper part of the deposit also contains large lenses of manganese oxides, principally pyrolusite and hausmannite. The presence of manganese with small amounts of copper, zinc, bismuth, silver, phosphorous, arsenic and other elements has led to an unusually diverse mineralogy. Collecting from the 1960s to the 1990s has resulted in more than 160 mineral species being recorded (Francis, 2010), and to date, six new mineral species have been described from Iron Monarch. Specimens of the new mineral species middlebackite were recovered from a one metre-sized quartz boulder found on RL160, on the southern side of the quarry in June 1990 (Francis, 2010). The boulder is considered most probably to have originated from RL247 about one metre below surface. Initial investigations of the mineral showed the presence of Cu and a trace of Zn and the powder x-ray pattern could not be

matched to any known mineral or synthetic compound. The mineral was mentioned as unnamed mineral UK05, a possible Cu carbonate or nitrate, by Pring *et al.* (2000) and Francis (2010). The recent structure refinement of the mineral using synchrotron X-ray diffraction data has enabled its full characterisation as a new Cu oxalate species. The mineral and its name have been approved by the International Mineralogical Association Commission of New Minerals, Nomenclature and Classification (IMA2015-115; Elliott, 2016). Holotype material is preserved in the South Australian Museum, Adelaide, South Australia (Registration number G34300). The mineral is named for the Middleback Range, in which Iron Monarch is situated.

Occurrence

Iron Monarch is a large sedimentary iron ore deposit of Precambrian age. During its geological history the deposit has been folded gently and intruded by dolerite dykes. The secondary minerals at Iron Monarch have formed during Tertiary and post-Tertiary weathering of the deposit at low temperature due to the interaction of basic fluids with hausmannite under changing pH conditions (Pring and Birch, 1993). These elements were mobilised into groundwaters during weathering processes. The secondary minerals precipitated from these fluids into fractures and joint planes in the orebody. The quartz boulder that contained the middlebackite has yielded a total of 50 mineral species, including sulfides (bornite, chalcocite, chalcopyrite, covellite, bismuthinite, pyrite, galena and sphalerite) and secondary minerals of Cu, Zn, Pb and Bi. On the type specimen, middlebackite occurs in seams in a matrix composed

Fig. 1. Groups of middlebackite crystals (blue) associated with atacamite (green) on quartz. The field of view is 1.1 mm across. Specimen in private collection.

of quartz and minor goethite. Associated minerals are atacamite and mottramtite. Middlebackite has formed in a near surface environment at low temperature. A source of oxalate was probably decaying organic matter. Copper was derived from weathering of Cu sulfides with dissolution of Cu possibly facilitated by oxalic acid.

Appearance, physical and optical properties

Middlebackite forms as aggregates of blue prismatic crystals up to 0.3 mm across (Fig. 1). Individual crystals are up to 0.05 mm long. Crystals are translucent with a vitreous lustre. The mineral has a pale blue streak. The Mohs hardness is ∼2. Crystals of middlebackite are brittle with one perfect cleavage and uneven fracture. The density could not be measured due to the limited availability of material. The calculated density is 3.64 g cm^{-3} based on the empirical formula. Optically, middlebackite is biaxial (+), with $\alpha = 1.663(4)$, $\beta = 1.748(4)$ and $\gamma = 1.861(4)$ (measured in white light). The calculated 2V is 86.7°. Dispersion is slight, $r > v$. The mineral is pleochroic with X = colourless, Y = very pale blue and Z = dark sky blue; $Z > Y > X$. The Gladstone–Dale compatibility, $1 - (K_P/K_C)$, is 0.011 based upon the empirical formula, in the range of superior compatibility (Mandarino, 1981).

Infrared spectroscopy

The infrared (IR) spectrum (Fig. 2) of powdered middlebackite in the range 4000 to 650 cm^{-1} was obtained using a Nicolet 5700
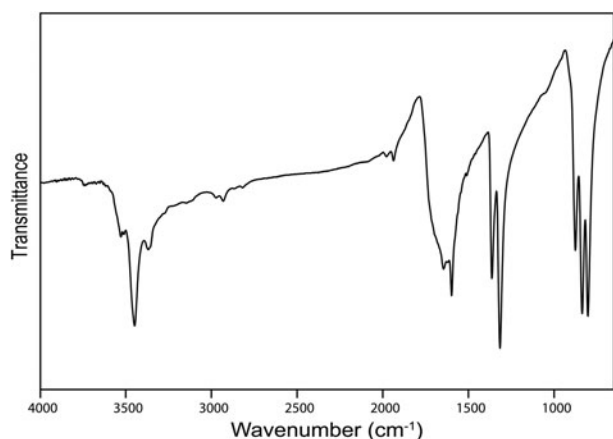

Fig. 2. The Fourier-transform IR spectrum of powdered middlebackite.

Table 1. Compositional data for middlebackite.

Constituent	Wt.%	Range	S.D.
CuO	64.18	59.96–69.00	3.07
ZnO	0.16	0.05–0.24	0.07
FeO	0.07	0.02–0.14	0.05
C$_2$O$_3$*	28.91		
P$_2$O$_5$	0.1	0.04–0.16	0.05
Cl	0.35	0.06–0.67	0.20
H$_2$O*	7.23		
O = Cl	−0.08		
Total	100.92		

Note: Number of analyses = 6; S.D. – standard deviation
* C$_2$O$_3$ and H$_2$O calculated from the ideal formula.

FTIR spectrometer equipped with a Nicolet Continuum IR microscope and a diamond-anvil cell. The IR spectrum of middlebackite demonstrates strong bands due to carboxylate groups. Bands at 1599 cm^{-1} and 1645 cm^{-1} can be assigned to in-phase and out-of-phase antisymmetric stretching vibrations of carboxylate groups and bands at 1365 and 1316 cm^{-1} to their in-phase and out-of-phase symmetric stretching vibrations. Bands in the range 800 to 900 cm^{-1} may be assigned to in-plane bending vibrations of carboxylate groups. The observation of three bands, at 876, 835 and 804 cm^{-1}, instead of the two expected due to the oxalate anion having two bending degrees of freedom suggests that one band could be assigned to Cu⋯O–H bending vibrations. Weak bands in the range from 1800 to 3200 cm^{-1} may correspond to overtones and combination modes. The spectrum shows a prominent sharp peak at 3448 cm^{-1} that can be attributed to the ν O–H stretching vibration of the hydrogen-bonded OH group. According to the empirical relation given by Libowitzky (1999), this frequency corresponds to a donor–acceptor O⋯O separation of ∼2.85 Å. The refined structure shows a separation of 2.890 Å. Smaller peaks at 3528, 3510 and 3369 cm^{-1} could represent overtones of carboxylate stretching vibrations.

Chemical analysis

Chemical analyses were carried out using a Cameca SXFive electron microprobe (energy dispersive spectroscopy mode, 15 kV,

Table 2. Powder X-ray diffraction data for middlebackite.

I_{obs}	I_{calc}	d_{obs}	d_{calc}	$h\,k\,l$	I_{obs}	I_{calc}	d_{obs}	d_{calc}	$h\,k\,l$
16	9	**7.070**	**7.037**	**1 0 0**	9	10	2.350	2.346	**3 0 0**
	1		4.450	1 1 0		3	2.218	2.225	2 2 0
4	3	3.934	3.971	0 1 $\bar{1}$	2	3	2.200	2.202	3 1 $\bar{1}$
100	100	**3.739**	**3.763**	**1 1 $\bar{1}$**	2	3	2.193	2.188	1 1 2
3	3	3.531	3.519	2 0 0		3		2.057	3 0 $\bar{2}$
3	6	3.211	3.217	1 1 1	2	4	1.998	1.985	0 2 $\bar{2}$
	2	3.010	3.000	2 1 0	2	7	1.895	1.881	2 2 $\bar{2}$
7	10	**2.905**	**2.908**	**2 1 $\bar{1}$**	2	8	1.824	1.826	1 2 2
18	24	**2.860**	**2.872**	**0 2 0**	2	8	1.811	1.817	3 2 0
6	8	2.760	2.747	0 0 $\bar{2}$		8		1.797	1 1 $\bar{3}$
2	4	2.649	2.659	1 2 0		6		1.787	1 3 $\bar{1}$
2	3	2.538	2.545	0 2 $\bar{1}$	6	12	1.749	1.745	0 1 $\bar{3}$
2	1	2.511	2.524	1 1 $\bar{2}$	6	14	1.733	1.729	4 1 $\bar{1}$
12	13	**2.481**	**2.488**	**1 2 $\bar{1}$**		3		1.672	3 2 $\bar{2}$
3	8	2.425	2.424	2 1 1		8		1.557	2 3 1
8	10	**2.373**	**2.366**	**1 0 2**					

Notes: Calculated intensities were obtained using the program *LAZY PULVERIX* (Yvon *et al.*, 1977); the strongest lines are given in bold.

Table 3. Crystal data, data collection and refinement details.

Crystal data

Ideal formula	$Cu_2C_2O_4(OH)_2$
Crystal dimensions (mm)	0.022 x 0.015 x 0.005
Crystal system, space group	$P2_1/c$
Temperature (K)	100
a, b, c (Å)	7.2597(15), 5.7145(11), 5.6624(11)
β (°)	104.20(3)
V (Å^3), Z	V = 227.73(8), 2
F(000)	240
μ (mm^{-1})	9.29
Calculated density (g cm^{-3})	3.64

Data collection

Diffractometer	ADSC Quantum 210r
Radiation, wavelength (Å)	Mo$K\alpha$, λ = 0.7108
Total no. of frames	360
θ range (°)	2.89–29.60
Absorption correction	SADABS (Bruker, 2001)
Detector distance (mm)	90.04
Rotation axes	ϕ
Rotation width (°)	1.0
Collection time per frame (s)	1
No. of measured, independent and observed [I >2$\sigma(I)$] reflections	4171, 627, 596
R_{int}	0.0515
Data completeness (%)	98.1
h, k, l ranges	$-9 \leq h \leq 9$, $-7 \leq k \leq 7$, $-7 \leq l \leq 7$

Refinement

Refinement on	F^2
R_1* for F_0 > 4$\sigma(F_0)$	3.41%
w$R_2^\dagger$ for all F_0^2	8.18%
Reflections used F_o > 4$\sigma(F_o)$	596
Number of parameters refined	55
Extinction factor	0.047(8)
$(\Delta/\sigma)_{max}$	0.000
GoF	0.819
$\Delta\rho_{min}, \Delta\rho_{max}$ (e^-/Å^3)	3.570,–0.704

*$R_1 = \Sigma||Fo| - |Fc|| / \Sigma|Fo|$
$^\dagger wR_2 = \Sigma w(|Fo|^2 - |Fc|^2)^2 / \Sigma w|Fo|^2)^{1/2}$; w = 1/[$\sigma^2(Fo^2)$ + (0.042 P)^2 + 12.60 P];
P = ([max of (0 or F_0^2)] + 2Fc^2)/ 3

15 nA and a defocused 20 μm beam diameter). The following standards and X-ray lines were used: almandine (Fe$K\alpha$), chalcopyrite (Cu$K\alpha$), willemite (Zn$K\alpha$) and apatite (P$K\alpha$). No additional element with atomic number $\geq$9 was detected in amounts >0.05 wt.% oxide. Data were processed using the ($\varphi\rho Z$) correction procedure of Pouchou and Pichoir (1985). Analytical data are given in Table 1. The presence of oxalate anions and OH were confirmed by infrared spectroscopy (Fig. 2) and by the crystal-structure analysis. The empirical formula, based on six oxygen atoms per formula unit, and with C_2O_3 and H_2O calculated from the ideal formula is $Cu_{2.00}(C_2O_4)Cl_{0.02}(OH)_{1.98}$. The simplified formula is $Cu_2C_2O_4(OH)_2$, which requires CuO 63.86, C_2O_3 28.91, H_2O 7.23; total 100.00 wt.%.

Table 5. Selected interatomic distances (Å), angles (°) and hydrogen bonds for middlebackite.

Cu–OH	1.939(2)	C–O1	1.257(3)	x 2
Cu–OH	1.964(2)	C–O2	<u>1.261(4)</u>	x 2
Cu–O1	1.971(2)	<C–O>	1.259	
Cu–O2	2.016(2)			
Cu–OH	2.397(2)	C–C	1.542(6)	
Cu–O2	<u>2.736(2)</u>			
<Cu–O>	2.171	C1–C1–O1	116.1(3)	x 2
		C1–C1–O2	117.0(3)	x 2
		O1–C1–O2	126.9(3)	x 2

Hydrogen bonds				
D–H$\cdots A$	D–H	H$\cdots A$	$D\cdots A$	$\angle D$–H$\cdots A$
OH–H1$\cdots$O2^i	0.87(4)	2.06(5)	2.890(3)	158(6)

Symmetry code: (i) $-x+1$, $-y+1$, $-z+1$.

Table 6. Bond valence* (valence units) details for middlebackite.

	Cu	C	H	Σ excluding H	Σ including H
O1	0.45	1.43		1.88	1.88
O2	0.40	1.42	0.15	1.88	2.03
	0.06				
OH	0.50		0.85	1.10	1.95
	0.46				
	0.14				
C		1.05			
Σ	2.01	3.90	1.00		

*Note: Bond-valence parameters used are from Brown and Altermatt (1985).

Powder X-ray diffraction

Powder X-ray diffraction data (Table 2) were collected using a Rigaku Hiflux Homelab diffractometer (Cu$K\alpha$ X-radiation, λ = 1.541870 Å). Calculated intensities were obtained from the structural model using the program *UNITCELL* (Holland and Redfern, 1997). Unit-cell parameters refined using the Le Bail profile-fitting method (Le Bail *et al.*, 1988, Hunter, 1998) and starting from the unit-cell parameters determined from the single-crystal study, are a = 7.282(1), b = 5.707(1), c = 5.693(1) Å, β = 104.51(2)° and V = 229.05(5) Å^3. These values show good agreement with the single-crystal values.

Structure determination

Single-crystal X-ray data collection and structure solution

Single-crystal X-ray diffraction data were obtained at the micro-focus macromolecular beam line MX2 of the Australian Synchrotron. Data were measured with an ADSC Quantum 210r detector using monochromatic Mo$K\alpha$ X-radiation (λ = 0.710800 Å), on a crystal 22 μm ×15 μm ×5 μm in size. A total of 4171 intensities were collected using a ϕ scan with frame

Table 4. Fractional atomic coordinates and displacement parameters (in Å^2) for for middlebackite.

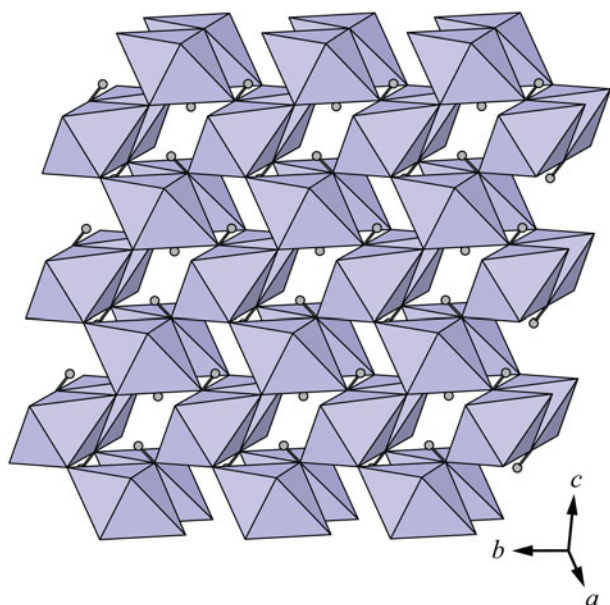| Atom	x	y	z	U_{eq}	U^{11}	U^{22}	U^{33}	U^{12}	U^{13}	U^{23}
Cu	0.66826(5)	0.52225(7)	0.19172(6)	0.0104(2)	0.0100(3)	0.0123(3)	0.0085(3)	0.00118(10)	0.00174(17)	−0.00093(11)
C	1.0436(4)	0.5680(5)	0.4093(5)	0.0114(9)	0.0129(15)	0.0100(14)	0.0116(14)	−0.0011(9)	0.0036(9)	−0.0010(10)
O1	0.9303(3)	0.6277(4)	0.2130(4)	0.0138(7)	0.0134(11)	0.0150(11)	0.0123(10)	0.0002(7)	0.0018(7)	−0.0001(7)
O2	0.7805(3)	0.3907(4)	0.5265(3)	0.0135(7)	0.0139(11)	0.0146(11)	0.0120(10)	0.0009(7)	0.0029(7)	−0.0001(7)
OH	0.4183(3)	0.3845(4)	0.1515(3)	0.0133(7)	0.0142(11)	0.0141(11)	0.0111(10)	0.0005(7)	0.0022(7)	0.0000(7)
H	0.367(9)	0.486(9)	0.230(11)	0.05						

Fig. 3. The sheet of $[CuO_3(OH)_3]$ octahedra in the crystal structure of middlebackite. All structure drawings were completed with *ATOMS* (Dowty, 1999).

widths of 1°, a counting time per frame of 1 s and a crystal-to-detector distance of 90.04 mm. The intensity data sets were processed using *XDS* (Kabsch, 2010) with absorption correction and scaling completed using *SADABS* (Bruker, 2001) resulting in 627 unique reflections, 596 of which were above $|F_o| > 4\sigma|F|$. Systematic absences were consistent with space group $P2_1/c$. The Cu atom was located during initial structure solution by direct methods using *SHELXS-97* (Sheldrick, 2015) within the *WinGX* program suite (Farrugia, 2012). The C atom and all O atoms were then located via subsequent difference-Fourier syntheses during the refinement, performed using *SHELXL-97* (Sheldrick, 2015). All sites refined to full occupancy. The position

of the H atom of the OH group were derived from difference-Fourier syntheses and its position refined freely with a fixed isotropic displacement ($U_{iso} = 0.05$). The final model with anisotropic-displacement parameters for all non-H atoms refined to an R_1 index of 3.41%. Details of data collection and structure refinement are provided in Table 3. Fractional coordinates and atom displacement parameters are provided in Table 4, selected interatomic distances in Table 5 and bond valences in Table 6. The crystallographic information file has been deposited with the Principal Editor of *Mineralogical Magazine* and is available as Supplementary material (see below).

Description of the crystal structure

The crystal structure of middlebackite (Fig. 3) comprises sheets consisting of edge- and corner-sharing octahedra parallel to the *bc* plane. $[CuO_3(OH)_3]$ octahedra share OH–OH edges to form $[Cu_2O_6(OH)_4]$ dimers. Dimers link via corners, through O2 and OH, along [011] and along [01$\bar{1}$]. Sheets link in the *a* direction via oxalate anions (Figs 4a and 7a). The Cu octahedron (Fig. 5) is strongly Jahn-Teller (4 + 2) distorted (Jahn and Teller, 1937; Eby and Hawthorne, 1993; Burns and Hawthorne, 1996) four short Cu–O bond lengths lie in the range 1.939 to 2.016 Å with apical O atoms at distances of 2.397 and 2.736 Å (Table 5). The bond-angle distortions are minor: the angle values showing the maximum deviations from the ideal 90 and 180° angles are 95.97 and 171.53°. The OH group is bonded to the Cu cation via two equatorial bonds and one apical bond. The H atom donates one hydrogen bond to the O2 anion at a distance of 2.06(5) Å and an OH–H1···O(2) angle of 158(6)°.

Discussion

Oxalic acid is ubiquitous in natural environments (e.g. Franceschi and Nakata, 2005; Fomina *et al.*, 2005) however, oxalate compounds are very rare in the geological environment. Oxalate
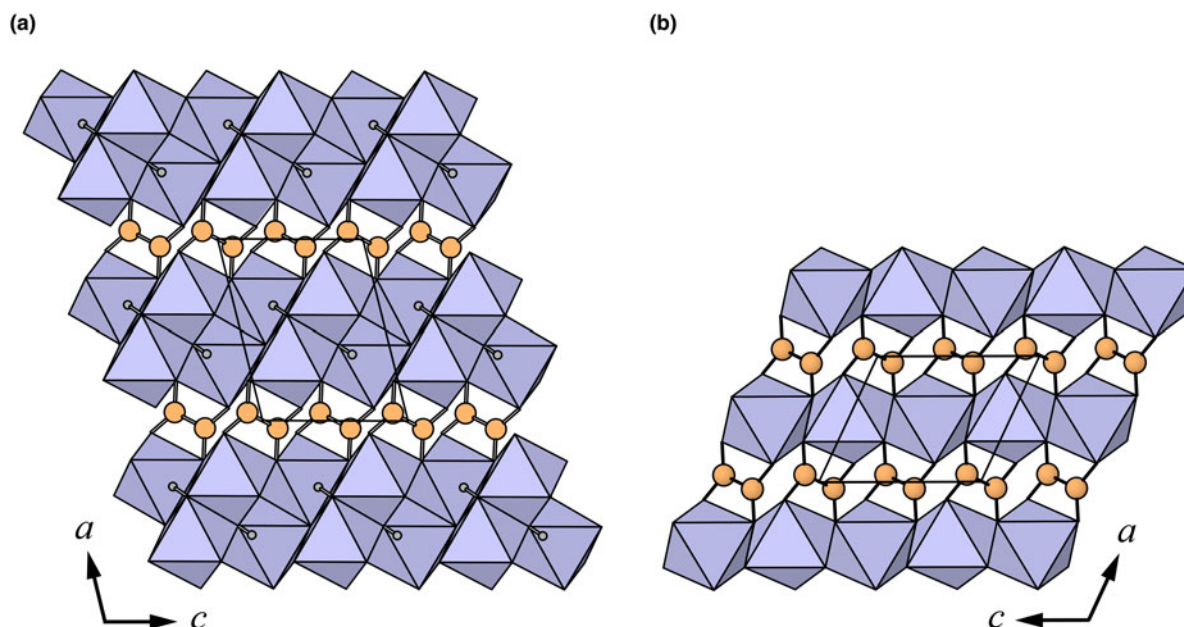

Fig. 4. The crystal structures of: (*a*) middlebackite; (*b*) moolooite viewed along [010]. The unit cells are outlined.
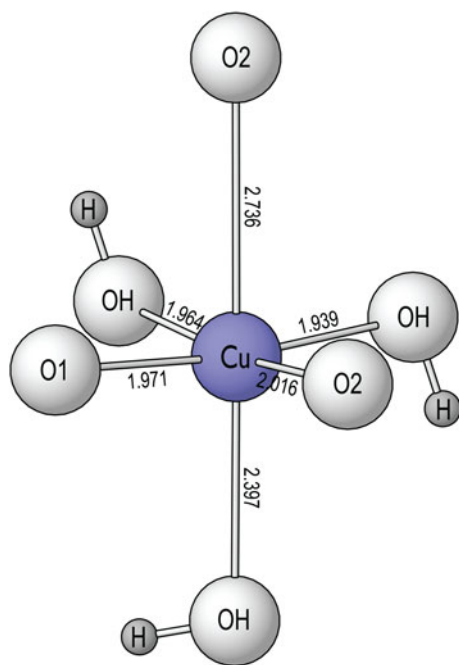
Fig. 5. Coordination of the Cu site in middlebackite showing Cu–O bond lengths in angstroms, Å.

Table 7. Comparison of crystallographic data for middlebackite and moolooite.

	Middlebackite	Moolooite Clarke and Williams (1986); Christensen et al. (2014)
Reference	This work	
Formula	$Cu_2C_2O_4(OH)_2$	$CuC_2O_4 \cdot nH_2O$
Crystal system	Monoclinic	Monoclinic
Space group	$P2_1/c$	$P2_1/n$
a (Å)	7.2597(15)	5.9569(2)
b (Å)	5.7145(11)	5.5528(1)
c (Å)	5.6624(11)	5.1247(1)
β (°)	104.20(3)	115.177(2)
V (Å^3)	227.73(8)	154.03(7)
Z	2	2
Strongest lines in the powder X-ray pattern	7.070(16), 3.739(100), 2.905(7), 2.860(18), 2.481(12), 2.373(8), 2.350(9)	3.88 (100), 2.50 (30), 2.33 (18), 2.31 (25), 2.14 (20), 1.787 (25), 1.753 (30)

minerals contain various cations such as Na, Ca, Al, Mg, transition metals and rare-earth elements. There are 20 minerals containing the oxalate anion, eight of which contain transition metals (Fe, Mn and Cu). Environments in which transition metal oxalate minerals occur include guano deposits, coal deposits, metal ore deposits and pegmatites. Middlebackite is the second Cu oxalate mineral after moolooite, CuC_2O_4, (Clarke and Williams, 1986; Christensen et al., 2014). Other Cu-bearing oxalates known in nature are antipinite, $KNa_3Cu_2(C_2O_4)_4$, (Chukanov et al., 2015) and wheatleyite, $Na_2Cu(C_2O_4)_2 \cdot 2H_2O$

(Rouse et al. 1986). Middlebackite is only the third known anhydrous oxalate mineral along with natroxalate, $Na_2(C_2O_4)$, (Khomyakov, 1996) and antipinite and is the only organic mineral to contain an OH group that is not part of a complex organic anion. Of the transition metal oxalate minerals, only middlebackite and antipinite have had their structures refined using natural material due to the difficulty in acquiring good-quality crystals.

The crystal structures of middlebackite and moolooite are closely related. Crystallographic data are given in Table 7. The structure of moolooite (synthetic) was refined from synchrotron powder X-ray and neutron powder diffraction data by Christensen et al. (2014). Both structures contain one Cu and one C site, however, whereas moolooite has two O sites, an additional OH site is present in the middlebackite structure. Calculation of bond-length distortion parameters (Renner and Lehmann, 1986) indicates that the Cu site in middlebackite is more strongly distorted than the site in moolooite with values of 12.704 and 9.872, respectively. The difference is mostly produced by the long apical bond Cu−O2 distance in middlebackite. Both structures are based on sheets of Cu octahedra. Linkage of
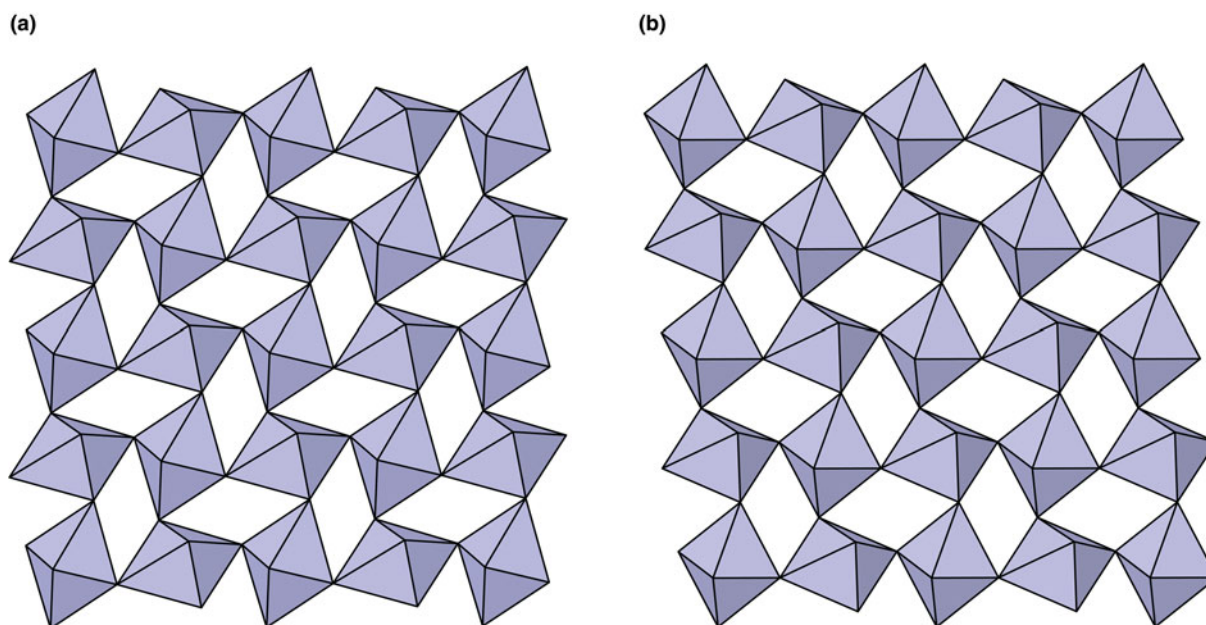

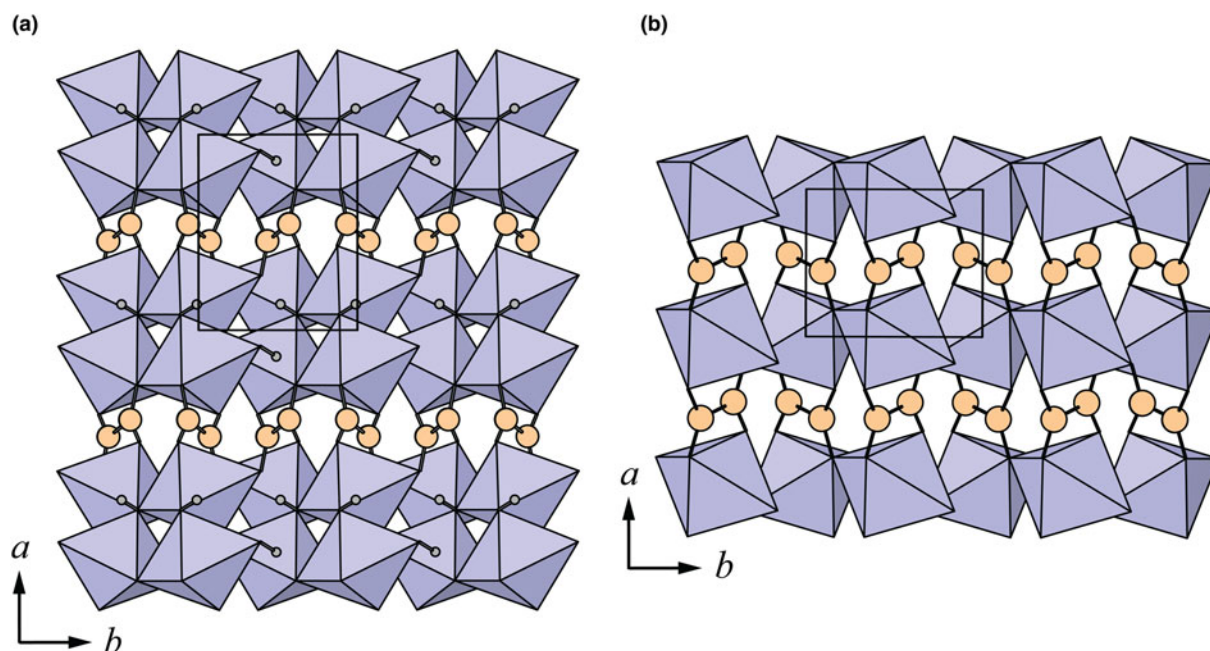Fig. 6. The crystal structures of: (a) middlebackite; (b) moolooite showing the linkage of octahedra in the bc plane.

Fig. 7. The crystal structures of: (*a*) middlebackite; (*b*) moolooite viewed along [001]. The unit cells are outlined.

the octahedra parallel to the sheet via corner-sharing is topologically identical in both structures (Figs 6). The structures differ, however, in that the sheet in middlebackite can be described as a double sheet, comprising two sheets linked via edge-sharing between octahedra. In both structures, linkage between sheets is via the C_2O_4 groups that link to the short O1–O2 edge of the Cu octahedron (Figs 4 and 7).

The Cu oxalate minerals moolooite and antipinite from their type localities were produced by the interaction of oxalic acids from guano with copper sulfide minerals (Clarke and Williams 1986; Chukanov *et al.*, 2015). The area in the Iron Monarch quarry that was most likely the source of the boulder that contained middlebackite was mined out many years ago (Francis, 2010) and the source of oxalate is not known for certain. The mineral was formed in a near surface environment and there are several possible sources of oxalate. Oxalate is produced by some plants, fungi and lichens (e.g. Dutton and Evans, 1996; Prieto *et al.*, 1997) and lichens and fungi living on mineral surfaces have been found to facilitate the dissolution of heavy metals (Chisholm *et al.* 1987; Fomina *et al.* 2005).

References

Brown I.D. and Altermatt D. (1985) Bond-valence parameters obtained by a systematic analysis of the Inorganic Crystal Structure Database *Acta Crystallographica*, **B41**, 244–247.

Bruker (2001) *SADABS*. Bruker AXS Inc., Madison, Wisconsin, USA.

Burns P.C. and Hawthorne F.C. (1996) Static and dynamic Jahn-Teller effects in Cu^{2+} oxysalts. *The Canadian Mineralogist*, **34**, 1089–1105.

Chisholm J.E., Jones G.C. and Purvis O.W. (1987) Hydrated copper oxalate, moolooite, in lichens. *Mineralogical Magazine*, **51**, 715–718.

Christensen A.N., Lebech B., Andersen N.H. and Grivel J-C. (2014) The crystal structure of paramagnetic copper (II) oxalate (CuC_2O_4) formation and thermal decomposition of randomly-stacked anisotropic nano-sized crystallites. *Dalton Transactions*, **43**, 16754–16768.

Chukanov N.V., Aksenov S.M., Rastsvetaeva R.K., Lyssenko K.A., Belakovskiy D.I., Färber G., Möhn G. and Van K.V. (2015) Antipinite, $KNa_3Cu_2(C_2O_4)_4$, a new mineral species from a guano deposit at Pabellón de Pica, Chile. *Mineralogical Magazine*, **79**, 1111–1121.

Clarke R.M. and Williams I.R. (1986) Moolooite, a naturally occurring hydrated copper oxalate from Western Australia. *Mineralogical Magazine*, **50**, 295–298.

Dowty E. (1999) *ATOMS for Windows and Macintosh. Version 5.0.6.* Shape Software, Kingsport, Tennessee, USA.

Dutton M.V. and Evans C.S. (1996) Oxalate production by fungi: its role in pathogenicity and ecology in the soil environment. *Canadian Journal of Microbiology*, **42**, 881–895.

Eby R.K. and Hawthorne F.C. (1993) Structural relationships in copper oxysalt minerals. I. Structural hierarchy. *Acta Crystallographica*, **B49**, 28–56.

Elliott P. (2016) Middlebackite, IMA 2015-115. CNMNC Newsletter No. 30, April 2016, page 411; *Mineralogical Magazine*, **80**, 407–413.

Farrugia L.J. (2012) WinGX and ORTEP for Windows: an update. *Journal of Applied Crystallography*, **45**, 849–854.

Fomina M., Hillier S., Charnock J.M., Melville K., Alexander I.J. and Gadd G.M. (2005) Role of oxalic acid overexcretion in transformations of toxic metal minerals by Beauveria caledonica. *Applied and Environmental Microbiology*, **71**, 371–381.

Franceschi V.R. and Nakata P.A. (2005) Calcium oxalate in plants: Formation and function. *Annual Review of Plant Biology*, **56**, 41–71.

Francis G.L. (2010) *Minerals of Iron Monarch*. OneSteel, Whyalla, South Australia, 165 pp.

Holland T.J.B. and Redfern S.A.T. (1997) Unit cell refinement from powder diffraction data: the use of regression diagnostics. *Mineralogical Magazine*, **61**, 65–77.

Hunter B.A. (1998) Rietica – A Visual Rietveld Program. *Commission on Powder Diffraction Newsletter*, **20**, 21.

Jahn H.A. and Teller E. (1937) Stability of polyatomic molecules in degenerate electronic states. *Proceedings of the Royal Society*, Series A, **161**, 220–236.

Kabsch W. (2010) XDS. *Acta Crystallographica*, **D66**, 125–132.

Khomyakov A.P. (1996) Natroxalate – $Na_2C_2O_4$ – a new mineral. *Zapiski Rossiiskogo Mineralogicheskogo Obshchestva*, **125**, 126–132 [in Russian].

Le Bail A., Duroy H., Fourquet J.L. (1988) Ab-initio structure determination of $LiSbWO_6$ by X-ray powder diffraction. *Materials Research Bulletin*, **23**, 447–452.

Libowitzky E. (1999) Correlation of O–H stretching ⋯O hydrogen bond lengths in minerals. *Monatshefte für Chemie*, **130**, 1047–1059.

Mandarino J.A. (1981) The Gladstone-Dale relationship: Part IV: The compatibility concept and its application. *The Canadian Mineralogist*, **19**, 441–450.

Milnes K.R. (1954) The geology and iron ore resources of the Middleback Range Area. *Geological Survey of South Ausralia, Bulletin*, **33**, 245 p.

Pouchou J.L. and Pichoir F. (1985) "PAP" (phi-rho-z) procedure for improved quantitative microanalysis. Pp. 104−106 in: *Microbeam Analysis* (J.T. Armstrong, editor). San Francisco Press, California, USA.

Prieto B., Silva B., Rivas T., Wierzchos J. and Ascaso C. (1997) Mineralogical transformation and neoformation in granite caused by the lichens *Tephromela atra* and *Ochrolechia parella*. *International Biodeterioration and Biodegradation*, **40**, 191–199.

Pring A. and Birch W.D. (1993) Gatehouseite, a new manganese hydroxy phosphate from Iron Monarch, South Australia. *Mineralogical Magazine*, **57**, 309–313.

Pring A., U. Kolitsch and G. Francis (2000) Additions to the mineralogy of the Iron Monarch deposit, Middleback Ranges, South Australia. *Australian Journal of Mineralogy*, **6**, 9–23.

Renner B. and Lehmann G. (1986) Correlation of angular and bond length distortions in TO_4 units in crystals. *Zeitschrift für Kristallographie*, **175**, 43–59.

Rouse R.C., Peacor D.R., Dunn P.J., Simmons W.B. and Newbury D. (1986) Wheatleyite, $Na_2Cu(C_2O_4)_2 \cdot 2H_2O$, a natural sodium copper salt of oxalic acid. *American Mineralogist*, **71**, 1240–1242.

Sheldrick G.M. (2015) Crystal Structure Refinement with SHELXL. *Acta Crystallographica*, **C71**, 3–8.

Yvon K., Jeitschko W. and Parthé E. (1977) LAZY PULVERIX, a computer program, for calculating X-ray and neutron diffraction powder patterns. *Journal of Applied Crystallography*, **10**, 73–74.